Published in final edited form as:
Chem Biol. 2009 September 25; 16(9): 1013–1020. doi:10.1016/j.chembiol.2009.08.009.

Sequential Reactions of Surface-Tethered Glycolytic Enzymes

Chinatsu Mukai[1], **Magnus Bergkvist**[2,3], **Jacquelyn L. Nelson**[1], and **Alexander J. Travis**[1,*]

[1]Baker Institute for Animal Health, College of Veterinary Medicine, Cornell University, Ithaca, NY 14853

[2]Nanobiotechnology Center, Cornell University, Ithaca, New York 14853

SUMMARY

The development of complex hybrid organic-inorganic devices faces several challenges, including how they can generate energy. Cells face similar challenges regarding local energy production. Mammalian sperm solve this problem by generating ATP down the flagellar principal piece by means of glycolytic enzymes, several of which are tethered to a cytoskeletal support via germ cell-specific targeting domains. Inspired by this design, we have produced recombinant hexokinase type 1 and glucose-6-phosphate isomerase capable of oriented immobilization on a nickel-nitrilotriacetic acid modified surface. Specific activities of enzymes tethered via this strategy were substantially higher than when randomly adsorbed. Furthermore, these enzymes showed sequential activities when tethered onto the same surface. This is the first demonstration of surface-tethered pathway components showing sequential enzymatic activities, and it provides a first step toward reconstitution of glycolysis on engineered hybrid devices.

INTRODUCTION

Hybrid organic-inorganic devices derive the potential benefits of combining biological functions with non-biological material systems. However, their practical development is faced with both functional and technical challenges. For example, a function that is desired for many devices is the ability to generate energy from available substrates.

Because adenosine triphosphate (ATP) supplies the power for many biological reactions, much attention has been focused on devices or systems that can produce their own ATP. Two systems to generate ATP have been reported that utilize the F_0F_1-ATP synthase (Luo et al., 2005; Steinberg-Yfrach et al., 1998). An alternative approach has been described that uses pyruvate kinase to generate ATP, which was used to power kinesin molecules (Du et al., 2005). These reports demonstrated that it is not only possible to engineer devices that

*Contact (corresponding Author): Alexander J. Travis, Baker Institute for Animal Health, College of Veterinary Medicine, Cornell University, Hungerford Hill Road, Ithaca, NY 14853, ajt32@cornell.edu office: 607-256-5613 fax: 607-256-5608.
[3]Present address: College of Nanoscale Science and Engineering, University at Albany, State University of New York, 255 Fuller Rd, Albany, NY 12203

can make ATP, but also that the ATP produced could be used to power desired molecular outputs. However, the F_0F_1-ATP synthase systems require exogenous light (photons), which is not practical for future *in vivo* medical applications. Similarly, the pyruvate kinase system relies on administration of phosphoenolpyruvate, which is also not freely available outside of cells. Thus, there are limitations when trying to translate these approaches into practical methods for local energy production, such as for medical devices that must function using substrates available in an organism.

Regardless of the end-goals of such devices, a technical obstacle common to the field is how to retain the activity of biological macromolecules while they are attached to a solid surface. To function properly, enzymes must have a conformation appropriate to engage with a substrate, they also must have access to that substrate, and when substrate is bound, many enzymes must change orientation or conformation in some fashion to carry out a reaction. Introducing specific domains or amino acid sequences in recombinant proteins is one strategy to tether them to a surface in an orderly fashion; however, the position and nature of such introduced sequences can greatly influence that protein's molecular function (Fischer and Hess, 2007; Halliwell et al., 2001; Tachibana et al., 2006). This challenge has important ramifications in biocatalysis, or the use of enzymes as part of chemical synthetic processes (Schoemaker et al., 2003). Difficulties associated with enzyme function on a solid phase have recently directed attention to the attachment of reaction *substrates* to solid supports (Basso et al., 2006; Laurent et al., 2008). However, this strategy is not suitable for technical applications such as those discussed above, because the enzymes would not naturally be found in the device's environment, unlike metabolizable substrates such as glucose.

In this manuscript, we seek to address the technical issue of maintaining protein function while bound to an inorganic support, in the context of reconstituting the first sequential steps in the metabolic pathway of glycolysis. This pathway converts glucose into pyruvate, releasing energy that can be used to form ATP. Biology can provide inspirations for solutions to these technical and functional challenges (Ummat A, 2005). For example, our work on mammalian sperm, along with that from other labs, has revealed how these cells have evolved variants of glycolytic enzymes that are bound to a solid, cytoskeletal structure known as the "fibrous sheath" (Cao et al., 2006; Krisfalusi et al., 2006; Storey and Kayne, 1975; Travis AJ, 2002; Westhoff and Kamp, 1997). These enzymes differ from their somatic counterparts in having domains that are believed to be involved in protein targeting to the fibrous sheath (Mori et al., 1998; Travis et al., 1998; Travis et al., 1999; Welch et al., 1992). This structure is found only in the flagellar principal piece, which is distal to the midpiece—the only region of sperm to contain mitochondria (Fig. 1). Thus, glycolysis can produce ATP locally where it is needed to power flagellar motility and the regulators of that motility (Miki et al., 2004; Mukai and Okuno, 2004; Travis et al., 2001).

The almost "solid-state" arrangement of glycolytic enzymes on the fibrous sheath of sperm inspired us to pursue a biomimetic strategy for oriented immobilization of these enzymes on inorganic supports. Namely, we hypothesized that replacement of a germ cell-specific domain with one that could promote binding to an inorganic support would result in an oriented immobilization that left the protein functional. This strategy therefore seeks to reduce the trial-and-error normally associated with this goal.

Using this biomimetic approach, the current manuscript describes the coupling and sequential activities of the first two enzymes of glycolysis when immobilized together on a single, solid support. Toward this goal, we generated recombinant forms of the male germ cell-specific hexokinase (HK: NM 010438; catalyzes the conversion of glucose to glucose-6-phosphate, utilizing ATP), and glucose-6-phosphate isomerase (GPI: NM 008155; catalyzes the conversion of glucose-6-phosphate to fructose-6-phosphate), and then tested their functions individually and in series on the same solid support. To our knowledge, we believe this to be the first demonstration of tethered pathway components showing sequential enzymatic activities, moving one step toward future hybrid organic-inorganic devices.

RESULTS

Generation of recombinant HK1 and GPI

The complementary deoxyribonucleic acid (cDNA) of a germ cell-specific isoform of HK1 (HK1-sc), and GPI were obtained by reverse transcription polymerase chain reaction (RT-PCR) from mouse testis ribonucleic acid (RNA), and the germ cell-specific targeting domain of HK (Travis et al., 1999) was removed by nested PCR. The constructs were inserted into a vector that places a hexahistidine (His-) tag at the amino terminus, thus replacing the HK1-sc germ cell-specific targeting domain. His-HK and His-GPI were expressed in a mammalian expression system and then purified using a nickel-nitrilotriacetic acid (Ni-NTA) system. The products were separated using sodium dodecyl sulfate polyacrylamide gel electrophoresis (SDS-PAGE) and their purity and identity were verified through the use of Coomassie staining and immunoblotting with antibodies against the respective proteins and against the His-tag. Both recombinant enzymes were found to be highly pure (80–90%, with only slight variations between sample preparations), immunoreactive with the appropriate antibodies, and to migrate at the expected molecular weights (Fig. 2).

Quantification of His-HK and His-GPI enzyme activities

We examined the activity of the recombinant proteins individually in solution by means of a coupled reaction pathway, ultimately measuring the reduction of nicotinamide adenine dinucleotide phosphate ($NADP^+$) by a change in absorbance at 340 nm. For both reactions, exogenous glucose-6-phosphate dehydrogenase (G6PDH) was added (see Materials and Methods below). We confirmed that the changes in absorbance specifically measured the target enzyme activities by running control reactions in the absence of exogenous G6PDH or substrate, and comparing the values from the experimental proteins versus commercially available purified HK1 and GPI.

His-HK demonstrated activity without the germ cell targeting region, with a V_{max} equal to 12 U/mg, and a K_m equal to 0.27 mM (glucose) (Table 1). These results were very similar to the values for the commercial HK enzyme in solution (V_{max} = 12 U/mg, K_m = 0.25 mM glucose). These results demonstrated that our recombinant HK remained functional with the germ cell-specific domain replaced by the hexahistidine-tag. We next evaluated the activity of His-HK when adsorbed to a 1 cm^2 gold surface modified to contain Ni-NTA groups (Fig. 3A). The recombinant showed activity on the surface, with negative controls being the

recombinant on the chip in the absence of the exogenous reaction components, and also a blank Ni-NTA chip in the presence of the reaction components. To identify the value of co-opting the germ cell-specific targeting domain, we made several attempts to generate a recombinant HK lacking either the native targeting domain or the His-tag (by means of the enterokinase site provided by the vector; data not shown). These proteins were highly labile and their degradation prevented us from obtaining interpretable comparative data.

We utilized a similar approach with His-GPI, which had a V_{max} equal to 49 U/mg, and a K_m equal to 0.23 mM (fructose 6-phosphate) when tested in solution (Table 1). Unlike the HK, we were able to utilize enterokinase (Novagen, EMD/Merck, Madison, WI) to remove the His-tag and still yield a stable protein. We used enterokinase resin and Ni-NTA agarose to remove the residual enterokinase and the protein from the cleaved His-tag, and verified there was no His-GPI remaining by means of SDS-PAGE and immuno-blotting using an antibody against the His-tag. After the cleavage, we measured the kinetic activity of the GPI protein and found similar results as prior to cleavage. The GPI construct without the His-tag had a V_{max} equal to 51 U/mg, and a K_m equal to 0.31 mM (fructose 6-phosphate). As with the HK, these values were very similar to those obtained for the commercial enzyme (V_{max} = 54 U/mg, K_m = 0.48 mM fructose 6-phosphate). Both experimental and control GPI recombinant proteins were stable for more than 2 months when stored at 4°C.

We next evaluated the activity of the His-GPI (Fig. 3B) when tethered to Ni-NTA gold surfaces. The recombinant showed activity when adsorbed to the surface, indicating that the protein was functional even when tethered. The adsorption and specific activities on the chips were significantly different between His-GPI and the control GPI, which had the His-tag removed with enterokinase (Fig. 4). Thus, the amino-terminal attachment not only facilitated a higher amount of total protein bound to the surface, but also significantly improved the activity of the protein that was adsorbed versus an equal amount adsorbed non-specifically.

His-HK and His-GPI reactions in series on a solid surface

After verifying the activities of the individual enzymes, we next mixed the recombinant His-HK and His-GPI in several different molar ratios and attached them to the same Ni-NTA modified surface. These two enzymes represent the first two sequential steps of glycolysis. After immobilization and thorough rinsing, we tested for sequential enzymatic activities of the tethered recombinant proteins. We found that the two enzymes did in fact act in series, metabolizing glucose into fructose 6-phosphate (Fig. 5). In our experiments, we found the His-HK protein to be rate-limiting (data not shown). Controls included adsorbing His-HK alone with the complete reagents for the coupled reaction pathway, and His-GPI alone with the complete reagents for the coupled reaction pathway, and with the buffer alone. All controls gave equivalent baseline readings (Fig. 5), confirming that the change in absorbance we observed did result from the sequential activities of the tethered enzymes. Only the two enzymes together showed activity under the coupled reaction pathway we employed. This demonstrated that the reaction buffer and its individual components were not contaminated with either of the enzymes, nor other chemicals that could cause a change in absorbance and a false-positive read out of sequential enzyme activities.

DISCUSSION

Tethering proteins to solid supports can interfere with function in several ways. The simple addition of a binding tag can induce folding errors that reduce activity (Halliwell et al., 2001), or can block sites critical for substrate or co-factor binding, or can prevent needed conformational changes. In the case of HK, which is well-characterized in terms of domain structure and function, one can appreciate the complexity of this problem. The approximately 100 kDa isoforms of this protein likely arose from a duplication and fusion event of an ancestral 50 kDa form, and catalytic function is associated with the C-terminus, whereas regulatory function is associated with the N-terminus (Wilson, 1997). Inappropriate placement of a fusion tag might interfere with ATP, glucose, or glucose-6-phosphate binding sites, the locations of which have been modeled based on data from crystals of the rat brain HK1 (Mulichak et al., 1998).

The N-terminal germ cell-specific sequence in HK1 that functions as a targeting domain (Mori et al., 1993; Travis et al., 1999) provides insight into how this protein could be tethered without retarding its function. Removal of the His-tag from His-HK resulted in an unstable protein, precluding comparisons of HK activity with and without the His-tag. However, His-HK had approximately the same activity in solution as the commercially available enzyme, demonstrating that replacement of the targeting domain with the His-tag was not significantly detrimental to its function. Copying the amino-terminal location of the germ cell-specific domain of HK proved effective for His-GPI as well. This recombinant protein showed almost a nine-fold improvement in specific activity when immobilized via the His-tag versus a control GPI without the His-tag that was randomly adsorbed to the surface.

Although an N-terminal germ cell-specific sequence has not to date been identified for GPI, differences in electrophoretic patterns for a germ cell variant have been reported (Buehr and McLaren, 1981). Other germ cell-specific glycolytic isozymes have been described that differ either in sequence, activity, or other characteristics for aldolase (Gillis and Tamblyn, 1984), triose-phosphate isomerase (Auer et al., 2004), glyceraldehyde 3-phosphate dehydrogenase (GAPD-S) (Welch et al., 1992), phosphoglycerate kinase (Boer et al., 1987), enolase (Edwards and Grootegoed, 1983), and pyruvate kinase (Feiden et al., 2007), as well as for the extra-glycolytic but related enzyme lactate dehydrogenase (LDH-C4) (Zhong and Kleene, 1999) (Zinkham, 1968).

Molecular characterization of these isozymes to identify potential germ cell-specific targeting domains might be of practical use in recapitulating the full glycolytic pathway on hybrid organic-inorganic devices. Completion of a functional, immobilized glycolytic pathway might facilitate the development of internal medical applications for hybrid devices, because they might one day be able to generate their own ATP locally from circulating glucose. Until that time, the present success with the first two enzymes of the pathway should provide a model system for the study of various questions related to enzyme activity on surfaces. For example, the resolution of lithographic patterning has made rapid advancements, and having enzymes that can function in series will allow for the study of how patterning might impact the efficiency of diffusion or substrate channelling.

SIGNIFICANCE

To the best of our knowledge, these data represent the first demonstration that sequential steps of a biological pathway can be replicated by proteins acting in series while anchored to a single, solid support. The pathway in question, glycolysis, metabolizes glucose to pyruvate, releasing energy that can be used to produce ATP. Thus, although these first steps actually consume ATP, should the rest of the glycolytic enzymes be reconstituted on a single device in the future, such a system could utilize circulating glucose as a metabolic substrate to generate ATP for a variety of functions. This would be of practical importance for the development of technical applications such as hybrid organic-inorganic medical devices. Progress toward such goals is limited by technical challenges; for example, tethering proteins to a support can interfere with function in a number of ways. This obstacle was overcome by mimicking the design of sperm, in which specific isoforms of glycolytic enzymes are bound to the fibrous sheath, and thus naturally attached to a solid interface. Knowledge of the germ cell-specific targeting domain of HK1-sc allowed identification of a site through which HK could be immobilized and still retain function. Recombinant His-HK and His-GPI were active individually and in series, with the activity of His-HK proving to be rate-limiting. His-GPI immobilized using this oriented attachment chemistry had a significantly higher specific activity than did GPI that was randomly adsorbed to the surface, demonstrating the importance of oriented immobilization. Additional work will be needed to generate and test other pathway components, and also to determine the optimal ratios and patterning of the enzymes to maximize flux through the system and minimize the diffusion of metabolic intermediates.

EXPERIMENTAL PROCEDURES

Generation of Recombinant Hexokinase and Glucose-6-Phosphate Isomerase

Full-length HK1-sc and somatic GPI were cloned from mouse testis by RT-PCR using the following primers, 5′-ATGGGACAGAACTGCCAGCGAGGAC-3′ (forward, HK1-sc), 5′-TTAGGCGTTCGTAGGGTCTCCTCTGAGCC-3′ (reverse, HK1-sc), 5′-ATGGCTGCGCTCACCCGGAACC-3′ (forward, GPI), and 5′-TTATTCTAGTTTGGTGTCCCGCTGTTGC-3′ (reverse, GPI). The germ cell-specific targeting domain of HK1-sc was removed by nested PCR using another forward primer, 5′-GAAAAGATTGATAAGTATCTGTATGCCATGCGGC-3′. HK and GPI cDNA were cloned into the expression vector pcDNA4/HisMax TOPO TA (Invitrogen, Carlsbad, CA), which added a 6 histidine repeat on the amino terminus, followed by an enterokinase cleavage site and then the glycolytic enzyme's sequence. Constructs were validated by sequencing and then were transfected into HEK293-F-FreeStyle cells (Invitrogen), using the 293fectin™ transfection reagent (Invitrogen). The protein was purified from cell lysates 48h later using a Ni-NTA purification system (Invitrogen). The purified proteins were dialyzed 3 times with 1L of 50 mM MOPS, and then concentrated using Amicon filtration centritubes (Millipore, Billerica, MA). Protein concentrations were determined with the Micro-BCA assay (Pierce, Rockford, IL), and purity of the samples was analyzed by SDS-PAGE and immunoblotting. The primary antibodies used were as follows: mouse anti-His tag (1:5000 dilution, Invitrogen), mouse anti-type1 hexokinase (1:1000 dilution, Chemicon, Temecula,

CA), and rabbit anti-GPI (1:500 dilution, Santa Cruz Biotechnology, Santa Cruz, CA). The secondary antibodies used were ECL anti-mouse IgG and ECL anti-rabbit IgG, both conjugated with horseradish peroxidase (Amersham, GE Healthcare, Piscataway, NJ).

Preparation of Ni-NTA Surface

Sulfuric acid (H_2SO_4), 30% hydrogen peroxide (H_2O_2), *N*-methyl-2-pyrrolidone, 16-mercaptohexadecanoic acid (MHA), ethanol, trifluoroacetic anhydride (TFA), triethylamine (TEA), *N*, *N*-dimethylformamide (DMF), tetrahydrofuran (THF), sodium hydroxide (NaOH), ethylenediaminetetraacetic acid (EDTA), nickel chloride ($NiCl_2$), *N*, *N*-bis-(carboxymethyl)-L-lysine-hydrate (NTA), triethylene glycol, and all other reagents were purchased from Sigma-Aldrich (St. Louis, MO) unless otherwise indicated. Gold surfaces (10/100 nm Cr/Au deposited on silicon by electron-beam evaporation) were made functional with Ni-NTA for the immobilization of His-tagged proteins as described previously (Yan et al., 1997) with some modifications. Briefly, gold surfaces were cleaned by incubating in a mixture of 2:1 H_2SO_4:H_2O_2 (Caution! Highly corrosive/oxidizing solution) for 5 min, followed by rinsing with deionized water and then ethanol. Samples were immediately immersed in an ethanol solution containing 2 mM MHA and incubated overnight (~16 hr). Control surfaces were incubated in ethanol without MHA. After incubation the surfaces were rinsed with ethanol, blown dry with high purity nitrogen (99.999%), and subsequently immersed in a solution of 100 mM TFA and 200 mM TEA in anhydrous DMF for 30 min. After the reaction (in which interchain anhydrides were formed), surfaces were rinsed thoroughly with DMF, blown dry with nitrogen, and immediately immersed in a solution containing 10 mM NTA, 10 mM triethylene glycol, and 7.5 mM NaOH at room temperature for 30 min. The surfaces were then rinsed with deionized water and blown dry under a stream of nitrogen. Ni-NTA activation was performed by immersing the gold surface in a solution of 40 mM $NiCl_2$ at room temperature for 2 h. Finally, the functionalized gold surface was rinsed thoroughly with deionized water, dried with nitrogen, and cut into pieces (~1 cm^2) using a diamond-tipped stylus.

Spectrophotometric Analysis of His-HK and His-GPI activity

HK and GPI activities were measured by means of coupled enzyme reaction pathways that led to the reduction of $NADP^+$ to NADPH. The rate of this reduction was measured as a change in absorbance at 340 nm using a spectrophotometer (SAFIRE microplate reader, Tecan, Medford, MA). The coupled reactions for HK were as follows: glucose + ATP $\rightarrow$ glucose-6-phosphate + ADP and glucose-6-phosphate + $NADP^+$ $\rightarrow$ NADPH + 6-phospho-glucono-δ-lactone, with the first reaction catalyzed by His-HK, and the second catalyzed by exogenous G6PDH. The coupled reactions for GPI were as follows: fructose-6-phosphate $\rightarrow$ glucose-6-phosphate and glucose-6-phosphate + $NADP^+$ $\rightarrow$ NADPH + 6-phospho-glucono-δ-lactone, with the first reaction catalyzed by His-GPI, and the second catalyzed by exogenous G6PDH. Fresh stocks of $NADP^+$ and ATP were prepared immediately prior to each trial. The base reaction mixture contained 1 mM $NADP^+$, 10 mM $MgCl_2$, and 3U/ml G6PDH in 50 mM MOPS buffer (pH 7.4). To quantify HK activity, 1 mM ATP and 5 mM glucose were added. To quantify GPI activity, 5 mM fructose 6-phosphate was added. Measurements of activity were determined from slopes taken from within the linear range. The K_m and V_{max} for each enzyme were calculated by quantifying the enzymatic activities

at various concentrations of their respective substrates and fitting the data to hyperbolic functions. One unit of enzyme activity was defined as the amount of enzyme that catalyzed the formation of 1 μmol of NADPH per min.

Tethering of enzymes to inorganic supports and quantification of activity while bound

To determine the amount of protein immobilized to the gold surfaces, we measured the protein concentration before and after surface adsorption using the Micro-BCA assay according to the manufacturer's instructions. The proteins were adsorbed by placing 60 μl of 50 mM MOPS (pH 7.4) containing known amounts of protein, at room temperature in the dark on a single gold Ni-NTA surface (1×1cm square). After 15 min, 50 μl of the solution was removed by pipetting, and 90 μl of the MOPS buffer was gently added to the surface. This volume was then collected and combined with the 50 μl that had been removed initially. The 140 μl was then analyzed to measure the amount of protein in solution that did not bind to the surface. Two more washes with 90 μl volumes of the MOPS buffer were performed, and these were also collected individually for quantification of protein that was removed. The amount of immobilized protein was calculated by subtracting the amount of protein found in the rinsing solutions from the initial starting amount. It should be noted that the amounts of protein removed by the second and third washes were consistently below the levels of detection. To ensure that all unbound or loosely bound protein was removed, the surface was then gently washed 3 times with 5 ml of MOPS buffer. Thus, it should be noted that for the purposes of quantification of specific activity, the amounts of protein actually bound were equal to or less than the amounts quantified, giving a conservative error in terms of specific activity.

To corroborate protein adsorption we measured the optical thickness before and after adsorption of the HK/GPI protein solution using imaging ellipsometry (SE-EP^3, Nanofilm, Goettingen, Germany). At least three different locations on a surface were measure and analysed. Film thickness values were calculated using a two layer optical model (layer 1 = substrate and layer 2 = organic film) using the Thinfilm Companion software (Semiconsoft, Boston, MA), where experimental data were fitted using a modified Marquardt-Levenberg minimization. The optical properties of the gold substrate (layer 1) were calculated using cleaned gold surfaces. Self-assembled monolayers and protein layers (layer 2) were modelled using a refractive index (n, k) of n = 1.45 and k = 0. The optical thickness of HK/GPI (with or without the His-tag) adsorbed to a Ni-NTA surface is reported in Figure S1. Adsorbed His-tagged protein showed a thickness increase of ~3.2 nm compared to the Ni-NTA surface while the protein without the tag only measured a layer thickness of ~0.65 nm. We also rinsed the surfaces briefly with a 10 mM EDTA solution (pH 8) to evaluate desorption of immobilized His-tagged protein. The EDTA rinse resulted in a ~50% reduction of His-tagged protein layer thickness while non-His-tagged protein showed similar results as before rinsing. These results indicate that the proteins most likely were oriented on the surface via their His-tag and that the binding to some extent was reversible.

The enzyme reactions themselves were carried out in a well with the chip in a 1 ml volume of reaction mixture. The changes in absorbance at 340 nm at various time points were measured in 300 μl aliquots of reaction mixture that were removed and transferred to

another well within the plate. Readings were obtained using a spectrophotometer as above. One unit of enzyme activity was defined as the amount of enzyme that catalyzed the formation of 1 μmol of NADPH per min. All assays were performed at least 3 times, each with at least triplicate sets of chips. Negative controls included the Ni-NTA surface alone and the surface with adsorbed protein, but missing the exogenous substrate. When possible, comparative measurements were obtained using chips adsorbed with the His-tagged recombinants versus recombinants that had the His-tag removed by enterokinase cleavage.

To determine whether His-HK and His-GPI could act in series, the proteins were immobilized by placing 60 μl of mixed protein solution (0.5 nM His-HK, 0.5 nM His-GPI in 50 mM MOPS buffer, pH 7.4) at room temperature in the dark on a single gold Ni-NTA surface (1×1cm square). After 15 min, 50 μl of the protein solution was removed by pipetting, and a similar washing procedure and protein assay were performed as described above. The assay of the sequential reaction of HK–GPI was performed at room temperature by measuring the oxidation of NADH at 340 nm as a result of exogenous glycerol 3-phosphate dehydrogenase. The reaction was carried out in a similar fashion as those for HK and GPI individually, with the reaction mixture containing 50 mM MOPS, 5 mM glucose, 1mM ATP, 0.5 mM NADH, 2 mM $MgCl_2$, 0.5 U/ml phosphofructokinase, 0.5 U/ml aldolase, 7 U/ml triose phosphate isomerase, and 2 U/ml glycerol 3-phosphate dehydrogenase at pH 7.4. Fresh stocks of NADH and ATP were prepared immediately prior to each trial. One unit of coupled reaction activity was defined as the amount of enzyme that catalyzed the formation of 1 μmol of NAD^+ per min. All assays were performed at least 3 times, each with at least triplicate sets of chips. Negative controls included the Ni-NTA surface alone, the surface with both adsorbed proteins but missing the exogenous substrate, or His-HK and the pathway reagents, or His-GPI and the pathway reagents.

Supplementary Material

Refer to Web version on PubMed Central for supplementary material.

Acknowledgments

We thank Ms. Anita Hesser and Ms. Jane Miller for their outstanding administrative support. This work was primarily supported by an Innovation Award from the Cornell Institute for Biotechnology and Life Science Technologies, a NYSTAR Designated Center for Advanced Technology (A.J.T.); other support was provided by the Marilyn M. Simpson Faculty Career Development Award (A.J.T.); the National Institutes of Health R01-HD045664 (A.J.T.); and the faculty research awards program (FRAP-A) at the University of Albany (M.B.). Part of this work was performed using facilities and equipment supported by the STC Program of the National Science Foundation under Agreement No. ECS-9876771.

References

Auer J, Camoin L, Courtot AM, Hotellier F, De Almeida M. Evidence that P36, a human sperm acrosomal antigen involved in the fertilization process is triosephosphate isomerase. Molecular Reproduction and Development. 2004; 68:515–523. [PubMed: 15236338]

Basso A, Braiuca P, Ebert C, Gardossi L, Linda P. Properties and applications of supports for enzyme-mediated transformations in solid phase synthesis. J Chem Technol Biotechnol. 2006; 81:1626–1640.

Boer PH, Adra CN, Lau YF, McBurney MW. The testis-specific phosphoglycerate kinase gene pgk-2 is a recruited retroposon. Molecular and Cellular Biology. 1987; 7:3107–3112. [PubMed: 2823118]

Buehr M, McLaren A. An electrophoretically detectable modification of glucosephosphate isomerase in mouse spermatozoa. Journal of Reproduction and Fertility. 1981; 63:169–173. [PubMed: 7277315]

Cao W, Gerton GL, Moss SB. Proteomic profiling of accessory structures from the mouse sperm flagellum. Molecular Cell Proteomics. 2006; 5:801–810.

Du YZ, Hiratsuka Y, Taira S, Eguchi M, Uyeda TQ, Yumoto N, Kodaka M. Motor protein nano-biomachine powered by self-supplying ATP. Chem Commun (Camb). 2005; 16:2080–2082. [PubMed: 15846406]

Edwards YH, Grootegoed JA. A sperm-specific enolase. Journal of Reproduction and Fertility. 1983; 68:305–310. [PubMed: 6864646]

Feiden S, Stypa H, Wolfrum U, Wegener G, Kamp G. A novel pyruvate kinase (PK-S) from boar spermatozoa is localized at the fibrous sheath and the acrosome. Reproduction (Cambridge, England). 2007; 134:81–95.

Fischer T, Hess H. Materials chemistry challenges in the design of hybrid bionanodevices: supporting protein function within artificial environments. J Mater Chem. 2007; 17:943–951.

Gillis BA, Tamblyn TM. Association of bovine sperm aldolase with sperm subcellular components. Biology of Reproduction. 1984; 31:25–35. [PubMed: 6466757]

Halliwell CM, Morgan G, Ou CP, Cass AE. Introduction of a (poly)histidine tag in L-lactate dehydrogenase produces a mixture of active and inactive molecules. Analytical Biochemistry. 2001; 295:257–261. [PubMed: 11488630]

Krisfalusi M, Miki K, Magyar PL, O'Brien DA. Multiple glycolytic enzymes are tightly bound to the fibrous sheath of mouse spermatozoa. Biology of Reproduction. 2006; 75:270–278. [PubMed: 16687649]

Laurent N, Haddoub R, Flitsch SL. Enzyme catalysis on solid surfaces. Trends Biotechnol. 2008; 6:328–337. [PubMed: 18430479]

Luo TJ, Soong R, Lan E, Dunn B, Montemagno C. Photo-induced proton gradients and ATP biosynthesis produced by vesicles encapsulated in a silica matrix. Nature Materials. 2005; 4:220–224.

Miki K, Qu W, Goulding EH, Willis WD, Bunch DO, Strader LF, Perreault SD, Eddy EM, O'Brien DA. Glyceraldehyde 3-phosphate dehydrogenase-S, a sperm-specific glycolytic enzyme, is required for sperm motility and male fertility. Proceedings of the National Academy of Sciences of the United States of America. 2004; 101:16501–16506. [PubMed: 15546993]

Mori C, Nakamura N, Welch JE, Gotoh H, Goulding EH, Fujioka M, Eddy EM. Mouse spermatogenic cell-specific type 1 hexokinase (mHk1-s) transcripts are expressed by alternative splicing from the mHk1 gene and the HK1-S protein is localized mainly in the sperm tail. Molecular Reproduction and Development. 1998; 49:374–385. [PubMed: 9508088]

Mori C, Welch JE, Fulcher KD, O'Brien DA, Eddy EM. Unique hexokinase messenger ribonucleic acids lacking the porin-binding domain are developmentally expressed in mouse spermatogenic cells. Biology of Reproduction. 1993; 49:191–203. [PubMed: 8396993]

Mukai C, Okuno M. Glycolysis plays a major role for adenosine triphosphate supplementation in mouse sperm flagellar movement. Biology of Reproduction. 2004; 71:540–547. [PubMed: 15084484]

Mulichak AM, Wilson JE, Padmanabhan K, Garavito RM 7 . The structure of mammalian hexokinase-1. Nature Structural Biology. 1998; 5:555–560.

Schoemaker HE, Mink D, Wubbolts MG. Dispelling the myths--biocatalysis in industrial synthesis. Science. 2003; 299:1694–1697. [PubMed: 12637735]

Steinberg-Yfrach G, Rigaud JL, Durantini EN, Moore AL, Gust D, Moore TA. Light-driven production of ATP catalysed by F0F1-ATP synthase in an artificial photosynthetic membrane. Nature. 1998; 392:479–482. [PubMed: 9548252]

Storey BT, Kayne FJ. Energy metabolism of spermatozoa. V. The Embden-Myerhof pathway of glycolysis: activities of pathway enzymes in hypotonically treated rabbit epididymal spermatozoa. Fertility and Sterility. 1975; 26:1257–1265. [PubMed: 803042]

Tachibana S, Suzuki M, Asano Y. Application of an enzyme chip to the microquantification of l-phenylalanine. Analytical Biochemistry. 2006; 359:72–78. [PubMed: 17046706]

Travis AJ, Foster JA, Rosenbaum NA, Visconti PE, Gerton GL, Kopf GS, Moss SB. Targeting of a germ cell-specific type 1 hexokinase lacking a porin- binding domain to the mitochondria as well as to the head and fibrous sheath of murine spermatozoa. Molecular Biology of the Cell. 1998; 9:263–276. [PubMed: 9450953]

Travis AJ, Jorgez CJ, Merdiushev T, Jones BH, Dess DM, Diaz-Cueto L, Storey BT, Kopf GS, Moss SB. Functional relationships between capacitation-dependent cell signaling and compartmentalized metabolic pathways in murine spermatozoa. The Journal of Biological Chemistry. 2001; 276:7630–7636. [PubMed: 11115497]

Travis, AJ.; Kopf, GS. The spermatozoon as a machine: compartmentalized pathways bridge cellular structure and function. In: De Jonge, CJ.; Barratt, CL., editors. Assisted Reproductive Technology: Accomplishments and New Horizons. New York, NY, USA: Cambridge University Press; 2002. p. 26-39.

Travis AJ, Sui D, Riedel KD, Hofmann NR, Moss SB, Wilson JE, Kopf GS. A novel NH(2)-terminal, nonhydrophobic motif targets a male germ cell-specific hexokinase to the endoplasmic reticulum and plasma membrane. The Journal of Biological Chemistry. 1999; 274:34467–34475. [PubMed: 10567428]

Ummat, A.; Dubey, A.; Marvoidis, C. Bio-Nanorobotics: A field inspired by Nature. In: Bar-Cohen, Y., editor. Biomimetics: Biologically Inspired Technologies. Boca Raton, FL, USA: CRC Press; 2005. p. 201-227.

Welch JE, Schatte EC, O'Brien DA, Eddy EM. Expression of a glyceraldehyde 3-phosphate dehydrogenase gene specific to mouse spermatogenic cells. Biology of Reproduction. 1992; 46:869–878. [PubMed: 1375514]

Westhoff D, Kamp G. Glyceraldehyde 3-phosphate dehydrogenase is bound to the fibrous sheath of mammalian spermatozoa. Journal of Cell Science. 1997; 110:1821–1829. [PubMed: 9264469]

Wilson JE. An introduction to the isoenzymes of mammalian hexokinase types I–III. Biochem Soc Trans. 1997; 25:103–107. [PubMed: 9056852]

Yan L, Marzolin C, Terfort A, Whitesides G. Formation and Reaction of Interchain Carboxylic Anhydride Groups on Self-Assembled Monolayers on Gold. Langmuir. 1997; 13:6704–6712.

Zhong X, Kleene KC. cDNA copies of the testis-specific lactate dehydrogenase (LDH-C) mRNA are present in spermatogenic cells in mice, but processed pseudogenes are not derived from mRNAs that are expressed in haploid and late meiotic spermatogenic cells. Mamm Genome. 1999; 10:6–12. [PubMed: 9892725]

Zinkham WH. Lactate dehydrogenase isozymes of testis and sperm: biological and biochemical properties and genetic control. Annals of the New York Academy of Sciences. 1968; 151:598–610. [PubMed: 5251885]

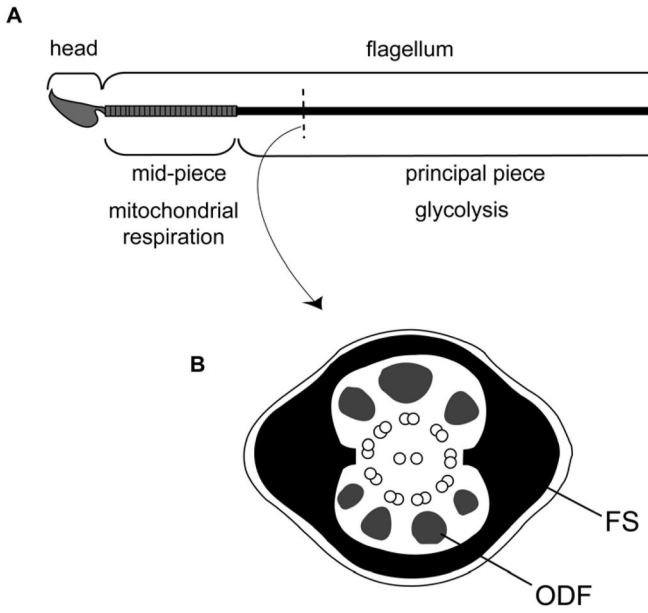

Figure 1.

Schematic diagram of murine sperm. (A) Sperm are highly polarized cells, divided into two main structural and functional units, the head and flagellum. The flagellum is further compartmentalized into the mid-piece, principal piece, and small terminal endpiece (not labelled). Oxidative phosphorylation is restricted to the mid-piece where mitochondria are located. The enzymes of glycolysis are located in the principal piece. (B) Cross section of principal piece. Mammalian sperm have accessory structures known as the outer dense fibers (ODF) and the fibrous sheath (FS), which both surround the central axoneme (9+2 microtubule doublets).

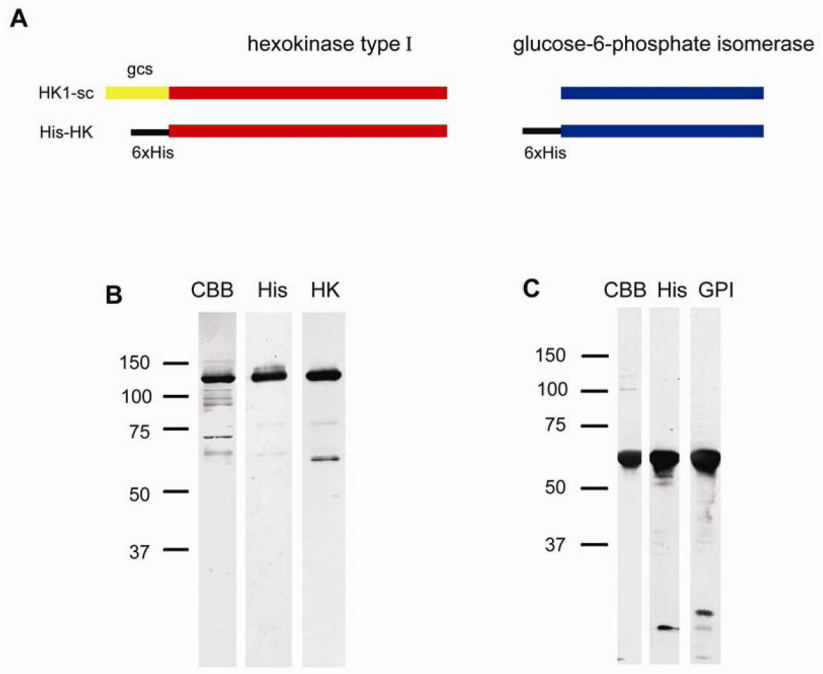

Figure 2.

Design of recombinant proteins and verification of purified His-HK and His-GPI. (A) Hexahistidine tags were introduced to the N-termini of HK and GPI. The known germ cell-specific targeting domain of HK1-sc was directly replaced by the His-tag. SDS-PAGE and immunoblot analysis of His-HK (B) and His-GPI (C) were performed as a quality control of the purification process and to verify the identity of the products. Coomassie brilliant blue (CBB) staining was performed to visualize the total proteins that were present at the end of purification. An antibody against the His tag (His) indicated the apparent molecular weights of proteins containing the tag, and antibodies against HK (HK) and GPI (GPI) were used to confirm the identity of the enzymes.

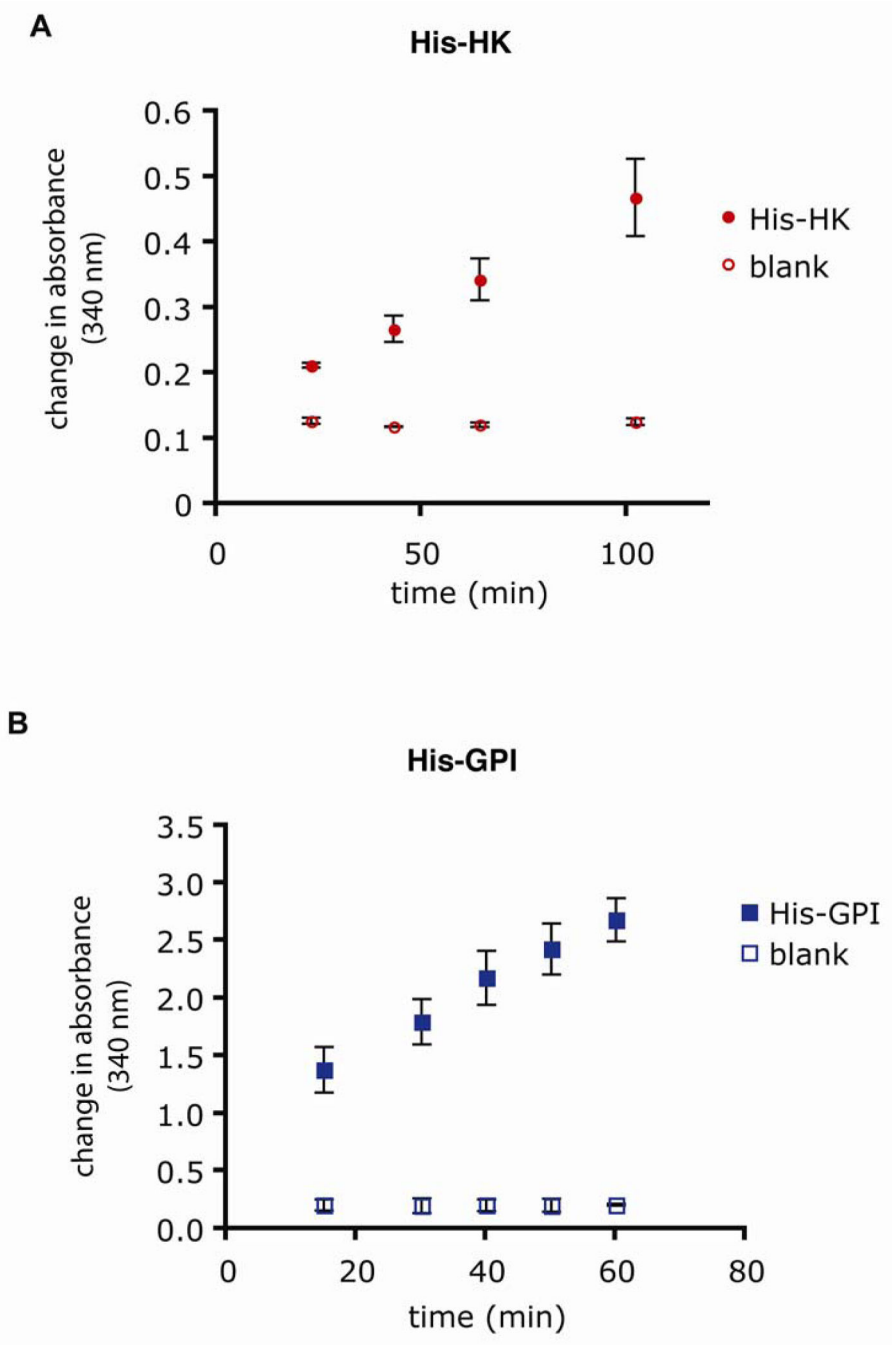

Figure 3.

Activities of bound His-HK and His-GPI when tethered individually. The recombinant proteins were tethered to gold chips with Ni-NTA surfaces, and washed well to remove any loosely bound or unbound proteins. Coupled enzymatic reactions were used to determine the activities of the proteins bound to the supports, with a change in absorbance at 340 nm measured spectrophotometrically, as described. Activities represent means from n = 9 samples, with 3 samples from each of 3 protein preparations. Bars indicate the standard deviations.).

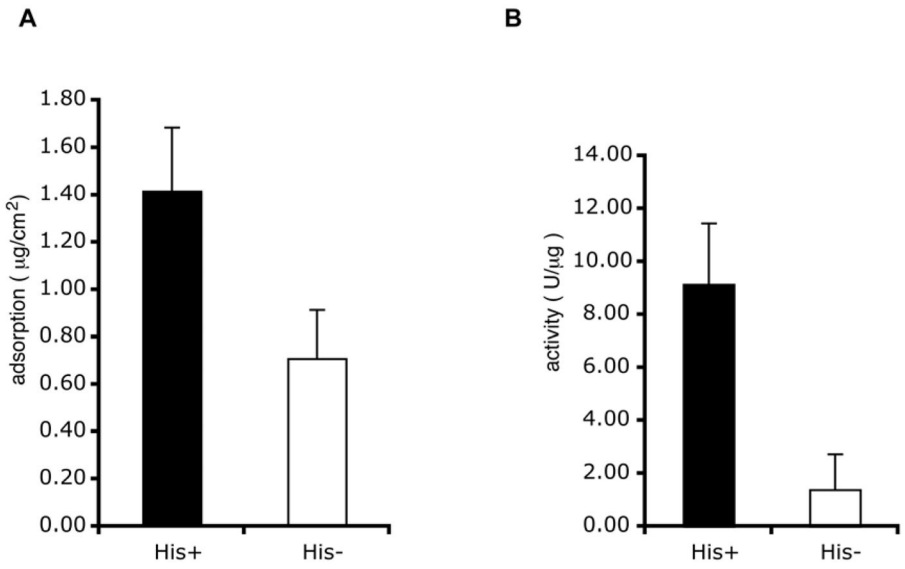

Figure 4.

Use of the amino terminal His-tag: Ni-NTA attachment chemistry improved binding and the specific activity of the GPI relative to GPI randomly adsorbed to the surface. The His-tag was cleaved from His-GPI by means of an enterokinase site provided by the vector. (A) Approximately twice as much His-GPI bound to a Ni-NTA support in comparison with control GPI lacking the His-tag (p=0.012, paired student T test; n = 9 samples, with 3 samples from each of 3 protein preparations. Bars indicate the standard deviations.). (B) Normalizing for the amount of protein bound allowed a quantification of the specific activities of the adsorbed proteins. The specific activity of the His-GPI was approximately 9 times greater than that of the randomly absorbed GPI, although the enzyme activities in solution were relatively equal (p=0.006, paired student T test; n = 9 samples, with 3 samples from each of 3 protein preparations. Bars indicate the standard deviations.).

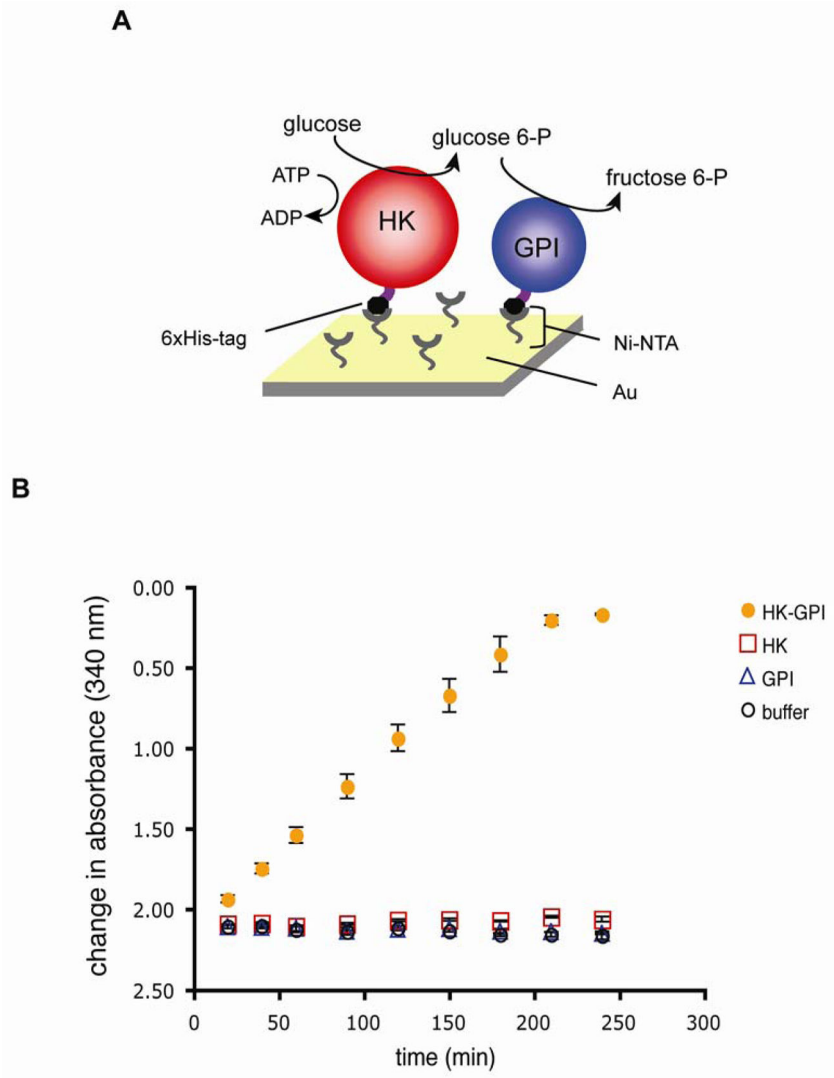

Figure 5.

Activity of His-HK and His-GPI in series on a single inorganic support. (A) Schematic diagram of surface chemistry, recombinant proteins, and the enzymatic reactions. The enzymes were immobilized to a solid support via the interaction of the His-tags with Ni-NTA. (B) His-HK and His-GPI were tethered together, allowing glucose to be catalyzed sequentially to glucose-6-phosphate and then to fructose-6-phosphate. Completion of the reaction was detected by the coupled reaction pathway as described. “HK-GPI” denotes supports incubated with 0.5 nM His-HK and 0.5 nM His-GPI. Readings for supports incubated with His-HK alone (HK) or His-GPI alone (GPI) were taken with protein solutions at 1nM concentration. A blank was performed with the Ni-NTA surface incubated in MOPS buffer (buffer). This figure is a representative result from one set of protein preparations, with triplicate samples (Bars denote standard deviations.). Because binding might be predicted to differ slightly for each protein for each set of preparations, it would

not be valid to pool the data for the experiments; however, the experiment was performed with three separate sets of preparations with very similar results each time.

Table 1

Properties of recombinant proteins. Enzyme activities in solution were determined as described. Values are for the substrates glucose (mM) for HK, and fructose 6-phosphate (mM) for GPI. The values shown are means ± SD (n = 3 protein preparations for each).

	V_{max}	K_m
His-HK	12 ± 5.8	0.27 ± 0.12
His-GPI	49 ± 8.9	0.23 ± 0.09